

# Green Synthesis of Gold Nanoparticles Mediated by *Garcinia* Fruits and Their Biological Applications

Azazahemad A. Kureshi<sup>1,2</sup>, Hiral M. Vaghela<sup>3</sup>, Satyanshu Kumar<sup>2</sup>, Raghuraj Singh<sup>2</sup>, Premlata Kumari<sup>1\*</sup>

<sup>1</sup>Applied Chemistry Department, Sardar Vallabhbhai National Institute of Technology, Surat - 395007, India.

<sup>2</sup>Organic Chemistry, Directorate of Medicinal and Aromatic Plants Research, Anand - 387310, India.

<sup>3</sup>Department of Chemistry, Government Science College, Gandhinagar - 382016, India.

## Article Info

### Article History:

Received: 12 August 2020

Accepted: 27 October 2020

ePublished: 12 January 2021

### Keywords:

-*Garcinia*  
-Extract  
-AuNPs  
-Antioxidant  
-Cytotoxicity

## Abstract

**Background:** Green synthesis of gold nanoparticles (AuNPs) using medicinal plant extract is an emerging area of research due to their applicability in nanomedicines.

**Methods:** In this study, aqueous extracts prepared from fruit-pericarps of two *Garcinia* species, *G. indica* (GI) and *G. cambogia* (GC) fruits which are important medicinally and commercially have been utilized for the synthesis of AuNPs. Various analytical techniques were utilized to characterize the synthesized AuNPs. The synthesized AuNPs were investigated for their biological properties such as antioxidant activity using the (2,2-diphenyl-1-picrylhydrazyl) DPPH model, cytotoxicity against MCF-7 (breast) cancer cell line, and antibacterial activity against two bacterial strains viz. *B. subtilis* and *E. coli*.

**Results:** The absorption peak of the AuNPs was observed at 541 nm using UV-Visible spectroscopy. The high resolution – scanning electron microscopy images showed spherical with a triangular shape AuNPs and their average sizes were ranging from 2 – 10 nm and it was found to be in good agreement with the particle size of 8 – 11 nm determined using X-ray diffraction analysis. Fourier-transform infrared spectroscopy revealed that water-soluble biomolecules from the aqueous extracts of the *Garcinia* species played a crucial role in the formation of AuNPs. The synthesized AuNPs exhibited considerable cytotoxicity with IC<sub>50</sub> values 34.55 µg/ml (GI) and 35.69 µg/ml (GC) against the MCF-7 cancer cell line. Furthermore, synthesized AuNPs also demonstrated significant antioxidant and antibacterial properties comparable to the standards used.

**Conclusion:** AuNPs have been synthesized using a simple green approach. The synthesized AuNPs demonstrated promising cytotoxicity, antioxidant, and antibacterial properties.

## Introduction

Nanotechnology is a rapidly emerging field of science that plays a pivotal role in the development of metal nanoparticles (NPs) with higher quality.<sup>1-3</sup> Nanomaterial based products have a wide spectrum of applications in catalysis,<sup>4,5</sup> biology,<sup>6</sup> coating technology,<sup>7</sup> electrochemical,<sup>8</sup> biomedical science,<sup>9</sup> pharmaceuticals,<sup>10,11</sup> dye-sensitized solar cells,<sup>12</sup> fabrication of stainless steel,<sup>13</sup> and biosensors.<sup>14,15</sup> Their alluring physico-chemical properties rose from quantum confinement impacts and large reactive surfaces together with intriguing biological activities have been incredibly considered in past few years.<sup>16-18</sup> Typically metals such as copper, gold, palladium, platinum, and silver from the coinage family are used to synthesize NPs. NPs synthesis can be achieved using different chemical,<sup>19</sup> physical,<sup>20</sup> and electrochemical<sup>21</sup> methods. Considering the harmful effects that these methods could cause on the environment and humans,<sup>22,23</sup> researchers have focused on

non-toxic, environmentally benign green chemical routes for the synthesis of metal NPs. It has been recognized that microorganisms,<sup>24,25</sup> plants,<sup>26,27</sup> and algae<sup>28</sup> are potential biological agents and could be used in the synthesis of NPs. The green methods offer advantages, including one-pot synthesis and eliminate the external addition of reducing, stabilizing, or capping agents to the reaction.<sup>27,28</sup> Secondary metabolites such as flavonoids, alkaloids, terpenoids, and tannins present in the plants can efficiently act as reducing and capping agents.<sup>29</sup> The cytotoxic properties of AgNPs (silver NPs), and AuNPs against various carcinomatous cells provides medication for mutagenic ailments.<sup>30,31</sup> Besides, the growth of pathogenic microorganisms was proficiently inhibited by biogenically synthesized NPs using noble metals.<sup>32-34</sup> Moreover, the synthesis of NPs using plant extracts has been proven to be easy, safe, cheap, and non-toxic.<sup>35,36</sup> The stability of the NPs can

\*Corresponding Author: Premlata Kumari, E-mail: premlatakumari1@gmail.com

©2021 The Author(s). This is an open access article and applies the Creative Commons Attribution License (<http://creativecommons.org/licenses/by-nc/4.0/>), which permits unrestricted use, distribution, and reproduction in any medium, as long as the original authors and source are cited.

be upgraded by appropriate capping agents that furnish stability and flexibility for binding affinity of molecules. The nature of the capping agent controls the uptake of NPs into cells, subject to their physico-chemical properties.<sup>37</sup> AuNPs were synthesized exploiting aqueous fruit pericarp extracts of two species of *Garcinia* that is well known to have their characteristic phytochemicals with phenomenal biological properties. Extracts of *G. indica* and *G. cambogia* have different phytochemical compositions, therefore the AuNPs mediated from the fruit pericarp extracts of these plants would have different physico-chemical properties, which motivates the investigators to utilize these aqueous fruits pericarp extracts in the synthesis of AuNPs.

*Garcinia indica* and *Garcinia cambogia* are the important members of the genus *Garcinia* belonging to the Clusiaceae (Guttiferae) family. The genus *Garcinia* comprises 200 species and about 36 species occur in India.<sup>38</sup> *Garcinia* species are a reservoir of a group of secondary metabolites including phenolics, flavonoids, xanthenes, organic acids, polyisoprenylated benzophenones (PIBs), and lactones.<sup>39</sup> The fruits of *Garcinia* species are well-known for their tremendous anti-obesity activity and hypocholesterolemic factor due to the presence of a high amount of (-) - hydroxycitric acid (HCA).<sup>40</sup> GI is commonly known as Malabar tamarind and found in many commercially available weight-reducing herbal formulations as a key ingredient. Globally, it is distributed in the subtropical region of Malaysia, China, Philippines, and evergreen forests of southwest India. GI is one of the medicinally and commercially appreciated species from the same genus known as 'Kokum' in India. Kokum was originally found only in the western peninsular coastal regions and the Western Ghats in the states of Maharashtra, Goa, Karnataka, and Kerala, as well as parts of Eastern India in the states of West Bengal, Assam, and North Eastern Hill regions, but nowadays Kokum trees are found growing in other parts of peninsular India.<sup>41</sup> The fruits of GI contain HCA and garcinia acid which have anti-obesity and anticholesterol activities.<sup>42</sup> It has been reported that the fruit rinds of GI and GC contain 10 – 30% HCA.<sup>43</sup> Phytochemical studies have shown that rinds of GI contain the highest concentration of anthocyanins (2.4g /100 g of GI fruit) when compared with any other natural sources.<sup>44</sup> Other phytochemicals such as xanthenes, PIBs, phenolics, and flavonoids have also been reported in GI and GC fruit rind extracts. GI fruit rinds contain xanthone namely  $\gamma$ -mangostin (0.11 % w/w), PIBs namely xanthochymol (1.09 – 18.44 % w/w), and isoxanthochymol (0.07 – 3.07 % w/w) in extracts of various polarities. In case of GC fruit rinds, the content of  $\gamma$ -mangostin was 0.12 % w/w, xanthochymol (0.09 – 21.42 %), isoxanthochymol (0.03 – 0.89 % w/w) were reported.<sup>45</sup> GI fruit rind extracts contain 3.84 – 4.73 % total phenolics<sup>46</sup> and 1.43 % total flavonoids;<sup>47</sup> while GC fruit rind extracts 2.07 – 4.60 % phenolics<sup>46</sup> and 1.37 % total flavonoids.<sup>48</sup> Various phytochemical studies revealed that GI has a slightly higher concentration of phytochemicals than GC which may take part in the

bio-reduction of Au<sup>3+</sup> ions. Moreover, pericarps of these fruits are also used in curry preparation as a taste enhancer. The fruit rind has a wide spectrum of uses such as food preservative, flavoring agent, or food bulking agent<sup>49</sup> and as a traditional remedy to treat constipation, piles, rheumatism, oedema, irregular menstruation, intestinal parasites, and many liver disorders in many Asian countries.<sup>50</sup> There are few research articles available on the synthesis of NPs using different metals and *Garcinia* species namely, *G. mangostana* – (AgNPs,<sup>51,52</sup> AuNPs,<sup>53,54</sup> PtNPs - Platinum NPs<sup>55</sup>), *G. pedunculata* – (PdNPs-Palladium NPs),<sup>56</sup> *G. indica* – (AgNPs),<sup>57</sup> *G. mangostana* – (ZnONPs - Zinc Oxide NPs),<sup>58</sup> *G. imberti* – AgNPs.<sup>59</sup> Desai *et al.* reported the synthesis of AuNPs using *G. indica* fruit aqueous extracts with 20-30 nm size.<sup>60</sup> Syed *et al.*<sup>61</sup> reported the synthesis of AgNPs using GI aqueous extracts prepared from leaves and stem. Raghavendra *et al.*<sup>62</sup> synthesized ZnONPs using *G. gummi-gutta* seed extract. Rajan *et al.*<sup>63</sup> reported the synthesis of AuNPs using GC fruit extract with significant catalytic properties. Krishnaprabha and Pattabi also reported the synthesis of AuNPs utilizing GI fruit rind extract with catalytic characteristics. However, studies reported by Rajan, Krishnaprabha, and Pattabi did not explore any biological activities.<sup>63,64</sup> Present investigation provides in-depth insight regarding the effect of phytochemical composition on the physico-chemical properties of AuNPs. In the present studies, the synthesized AuNPs were investigated for their cytotoxicity potential, antioxidant, and antibacterial activities.

In the present investigations, we report a green synthesis of AuNPs using aqueous extracts of two abovementioned *Garcinia* species. Synthesized AuNPs were characterized by UV-Visible spectroscopy (UV-Vis), Fourier Transform Infrared spectroscopy (FT-IR), X-ray Diffraction (XRD), High-Resolution Transmission Electron Microscopy (HR-TEM), and Energy Dispersive X-ray spectroscopy (EDX). In addition to that, a comprehensive study was carried out to examine the antioxidant activity using DPPH free radical scavenging assay, and cytotoxicity properties of AuNPs against MCF-7 cancer cell line using MTT (3-[4, 5-dimethyl-2-thiazolyl]-2, 5-diphenyltetrazolium bromide) assay. Furthermore, antibacterial activity against two bacterial strains namely *B. subtilis* and *E. coli* were also carried out.

## Materials and Methods

Analytical grade Chlorauric acid was obtained from Sigma Aldrich (Mumbai, India). Authenticated fruit pericarp powder of GI and GC was procured from the local market. For the cytotoxicity studies, MCF-7 cell culture was obtained from NCCS (National Centre for Cell Science), Pune, Maharashtra, India. Dulbecco's Modified Eagles Medium (DMEM) and phosphate buffer solution (PBS) were procured from Gibco (USA) fetal bovine serum (FBS) obtained from Invitrogen (Karnataka, India).

### Preparation of aqueous extracts of GI and GC fruit pericarps

The purchased powder was grounded using an electric grinder to obtain a fine powder. 10 g of pericarp powder was added into a flask containing 100 ml triple distilled water and heated at 70°C for 30 minutes and filtered using Whatman No. 1 filter paper. The filtrate was stored at 4°C in the refrigerator for further use.

### Synthesis of AuNPs using aqueous extracts of GI and GC

In a conical flask, 20 ml of each extract was reacted with 1 mM of tetrachloraurate at 60°C on a magnetic stirrer with constant stirring for 30 minutes. The brownish color of the GI extract changed to a violet color indicating the formation of AuNPs/GI after an hour. The color formation in GC extract was orange to dark purple confirming the AuNPs/GC. The reduction of Au<sup>+3</sup> to Au<sup>0</sup> was due to the involvement phytoconstituents present in extracts which act as a reducing agent and capping agent. The color change in the reaction mixtures was observed and the AuNPs formation was confirmed using UV-Vis spectrometry. Furthermore, each mixture was allowed to centrifuge at 6000 rpm for 15 minutes to separate AuNPs from unwanted materials. Subsequently, synthesized AuNPs and the supernatant were reconstituted in triple distilled water. This procedure was repeated thrice and the purified AuNPs were dried under vacuum and characterized. To study the stability of synthesized AuNPs, the colloidal solution solutions were stored at 4°C in a refrigerator.

### Characterization of AuNPs

The UV-Visible spectrum of each synthesized AuNPs was monitored using a double beam spectrophotometer (Shimadzu 1800 UV-Visible spectrophotometer). The absorbance was measured in the wavelength range of 200-800 nm. Fourier transform infrared spectra were recorded using Shimadzu (FTIR-8400S) in transmission mode between 400-4000 cm<sup>-1</sup> range. The crystallographic analysis of AuNPs was determined by the X-ray diffractometer (Rigaku D/MAX diffractometer). Elemental analysis of synthesized AuNPs was performed using energy dispersive X-ray spectroscopy with field emission scanning electron microscopy (JEOL JSM-7600F). The study of the sizes and morphologies of the biogenically synthesized AuNPs has been performed on the Tecnai G2-F30 model high-resolution transmission electron microscopy. The average size of the synthesized AuNPs was measured.

### DPPH free radical scavenging activity

The free radical activities of the synthesized AuNPs were studied using DPPH assay.<sup>65-67</sup> One ml of test solution from extracts/AuNPs of different

concentrations (20-100 µg/ml) was mixed with 2 ml 0.1 mM DPPH methanolic solution. The reaction mixture was allowed to incubate for 30 minutes in the dark. The optical density (OD) was measured using a UV-Vis spectrophotometer at 517 nm. The antioxidant activity of the synthesized AuNPs can be expressed as a given formula in terms of (%) radical scavenging activity (RSA).<sup>68</sup> Ascorbic acid (20-100 µg/ml) was used as a standard.

$$\% \text{ RSA} = \left( \frac{\text{Control OD}_{517} - \text{Sample OD}_{517}}{\text{Control OD}_{517}} \right) * 100$$

### Cytotoxic activity

The cells were cultured in DMEM low glucose with glutamine supplemented with 10 % FBS, 5 % penicillin, and streptomycin. The cultures were incubated at 37°C in a humidified 5 % CO<sub>2</sub> atmosphere. To prevent aggregation, 20 minutes sonication was done before preparing the stock solution of 1000 µg/ml of AuNPs. Cell viability assay was determined using MTT assay as reported by Patil *et al.* with few modifications. MCF-7 cell lines were seeded in each well of a 96 – well culture plate (5 × 10<sup>4</sup> cells/ per 100 µl).<sup>27</sup> Cell cultures were incubated for 24 hours at 37°C and 6.5% CO<sub>2</sub>. After that, cells were treated with various concentrations (0.05-1000 µg/ml) of AuNPs<sup>3</sup> solutions. Then again cell cultures were incubated for 24 hours under the same conditions. 10 µl MTT solution (5 mg/ml in PBS) was added to each well, and incubated for 4 hours at 37°C. The resulted formazan crystals were solubilized by adding 150 µl DMSO. The OD was measured at 570 nm (reference wavelength 655 nm) using the ELISA reader (Thermo-Fisher Scientific, USA). A control was prepared without treatment. The efficacy of AuNPs on the MCF-7 cell lines was expressed as the % of cell viability using the following formula. The concentration causing 50 % cell growth inhibition (IC<sub>50</sub>) was determined from the dose-response curve using GraphPad Prism software (Ver. 5.04) (USA). The IC<sub>50</sub> value was calculated using the nonlinear regression program origin.

$$\% \text{ cell viability} = \left( \frac{\text{Sample OD}_{570}}{\text{Control OD}_{570}} \right) * 100$$

### Antibacterial activity

The antibacterial activities of synthesized AuNPs at different concentrations against bacterial strains, *viz.* *Escherichia coli* (MTCC 119) and *Bacillus subtilis* (MTCC 121), were determined by the agar well diffusion method.<sup>69-71</sup> The pathogenic bacteria used in the study were obtained from the Microbial Type Culture Collection and Gene Bank (MTCC), Chandigarh, India. Fresh overnight culture of each bacterial strain swabbed uniformly by cotton on plates containing sterile Muller Hinton Agar (MHA) and 4

well was prepared using a cup borer with a diameter size of 6 mm. 50  $\mu$ l of AuNPs synthesized from each plant was poured into each well and incubated the plates for 24 hours at 37°C, after the incubation period zone of inhibition (ZOI) was observed around each well with the diameter in millimeter. Gentamicin was used as a positive control.

## Results and Discussion

### Biogenic synthesis of AuNPs

The present investigation demonstrates the simple, rapid, and cost-effective green synthesis of AuNPs using fruit pericarp extracts of two important *Garcinia* species. These fruit pericarp extracts contain various phytochemical constituents such as organic acids, vitamins, amino acids, PIBs, xanthenes, phenolic, and flavonoids that could be responsible for the synthesis of AuNPs.<sup>54,62</sup> Various analytical techniques could confirm the formation of synthesized AuNPs.

### UV-Vis spectroscopic analysis

UV-Visible spectroscopy was used to determine the formation and stability of biogenic AuNPs. The color change from brown to violet in GI and orange to dark violet in GC was due to the surface plasmon resonance (SPR) band. Particle size, shape, and the reaction medium are the key components responsible for the SPR pattern.<sup>72</sup> Reports showed that in aqueous solution AuNPs exhibits violet color due to the excitation of surface plasmon vibrations phenomena in the metal NPs.<sup>73</sup> The SPR of the AuNPs involves two phenomena: scattering and absorption. The scattering phenomenon is known to be responsible for fluorescence enhancement and the absorption phenomenon fluorescence quenching.<sup>74</sup> AuNPs absorption band occurs around 541 nm (Figure 1). The stability of AuNPs was also checked after 13 months using UV-Vis spectroscopy (Figure 2). The

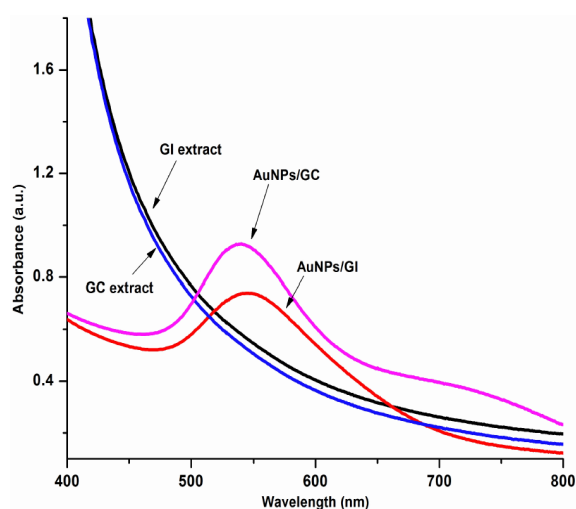


**Figure 1.** UV-Vis spectra of the synthesized AuNPs.

terminologies “Old” and “New” denote the UV-Vis spectra taken after 13 months and immediately after the preparation, respectively. The stability, size, and shape of the AuNPs are commonly affected by factors such as the concentration of plant extract and tetrachloraurate, pH, temperature, and exposure time. After a long period of 13 months, the synthesized NPs have neither completely degraded nor agglomerated.

### FT-IR analysis

FT-IR spectra of both extracts and AuNPs were performed to get information about extract constituents involved in the reduction of  $\text{Au}^{+3}$  to Au and/or stabilization of AuNPs. The FT-IR spectra are shown in Figure 3(a) and 3(b). The FT-IR spectra of extracts and AuNPs are very similar. Despite the similarity in the spectra of extracts and AuNPs, some absorption peaks exhibited shifts in their position and/or decrease in their intensity. The decrease in relative intensities and absorption frequencies at  $3369\text{ cm}^{-1}$  and  $3376\text{ cm}^{-1}$ ;  $1738\text{ cm}^{-1}$ ,  $1633\text{ cm}^{-1}$  and  $1077\text{ cm}^{-1}$  suggests the involvement of the biomolecules containing O-H groups (polyols), -C=O group (flavonoids), -C-N and -N-H (proteins) in bioreduction and/or in stabilizing NPs. The absorption peaks at  $2356\text{ cm}^{-1}$  and  $2357\text{ cm}^{-1}$  are due to atmospheric carbon dioxide.<sup>75</sup> The absorption peak shifts/decrease in intensity and their interpretation are shown in Table 1.

### X-ray diffraction analysis

XRD analysis plays a key role to define the phase structure and purity of the synthesized NPs. The XRD pattern for the AuNPs, synthesized utilizing aqueous extract of *Garcinia* shows intense diffraction peaks [Figure 4(a) and 4(b)] at  $2\theta$  (degrees) of  $38.13^\circ$ ,  $44.28^\circ$ ,  $64.52^\circ$ ,  $77.57^\circ$ , and  $81.69^\circ$  which corresponds to the (111), (200), (220), (311), and (222) (Joint Committee on Powder Diffraction Standard, JCPDS no. 01-1174)

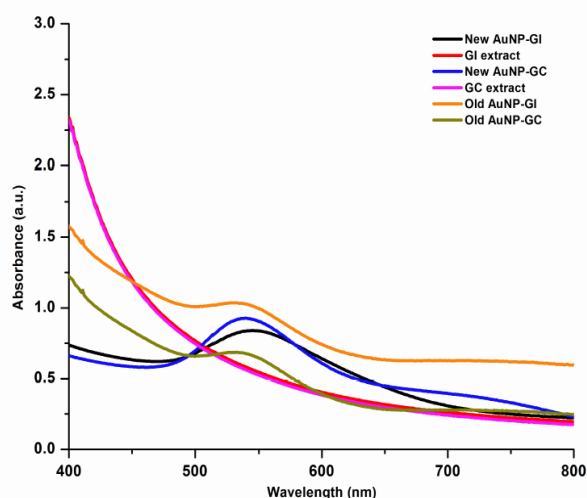


**Figure 2.** Comparison of UV-Vis spectra of AuNPs at two different time intervals.

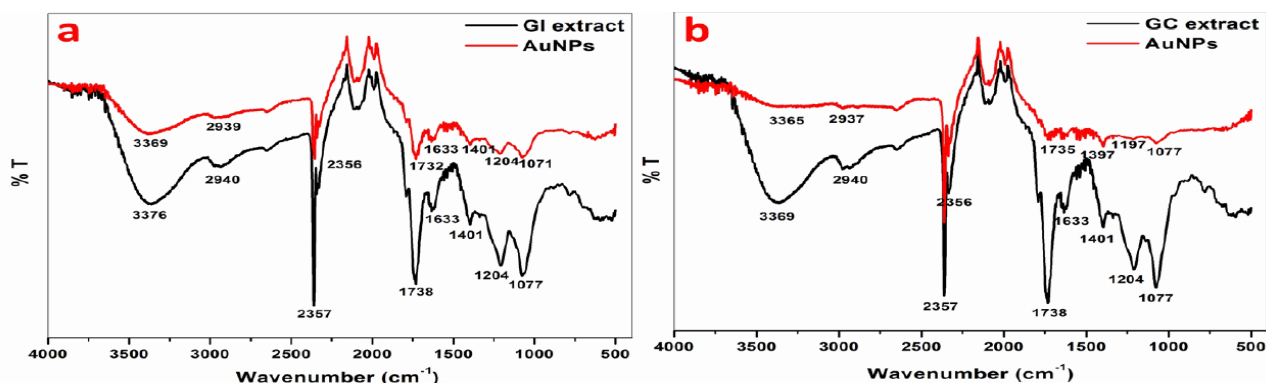


**Figure 3.** FT-IR spectra of the (a) AuNPs/GI and (b) AuNPs/GC.

**Table 1.** Significant absorption peaks with shift in their position/decrease in their intensity in the AuNPs with respect to the extracts.

| Extract source | Peaks in extract (cm <sup>-1</sup> ) | Peaks in AuNPs (cm <sup>-1</sup> ) | Types of chemical bond                              |
|----------------|--------------------------------------|------------------------------------|---|
| GI             | 3376                                 | 3369                               | O-H (alcohols/Phenols), N-H (amines/amides)         |
|                | 2940                                 | 2939                               | =C-H (alkenes)                                      |
|                | 2357                                 | 2356                               | Absorption doublet band of CO <sub>2</sub>          |
|                | 1738                                 | 1732                               | C=O (carboxylic acid/ester/flavonoids)              |
|                | 1633                                 | 1633                               | Decrease in intensity, C=C stretching, N-H bending  |
|                | 1401                                 | 1401                               | Decrease in intensity, C-H bending                  |
|                | 1204                                 | 1204                               | Decrease in intensity, O-CH <sub>3</sub> stretching |
|                | 1077                                 | 1071                               | C-O stretching                                      |
| GC             | 3369                                 | 3365                               | O-H (alcohols/Phenols), N-H (amines/amides)         |
|                | 2940                                 | 2937                               | =C-H (alkenes)                                      |
|                | 2357                                 | 2356                               | Absorption doublet band of CO <sub>2</sub>          |
|                | 1738                                 | 1735                               | C=O (carboxylic acid/ester/flavonoids)              |
|                | 1633                                 | 1633                               | decrease in intensity, C=C stretching, N-H bending  |
|                | 1401                                 | 1397                               | decrease in intensity, C-H bending                  |
|                | 1204                                 | 1197                               | decrease in intensity, O-CH <sub>3</sub> stretching |
|                | 1077                                 | 1077                               | decrease in intensity, C-O stretching               |

planes of Bragg reflections of face-centered cubic (FCC) structure of AuNPs. The intensity of the peaks further indicates that the synthesized AuNPs are of a high degree of crystallinity and hence the responsible phytochemicals can reduce Au<sup>3+</sup> and stabilize the

AuNPs formed. Following Debye-Scherrer formula was used to calculate an average particle size of the AuNPs:<sup>76,77</sup>

$$D = K\lambda / \beta \cos\theta$$

Where, D is the average crystalline size, K is the

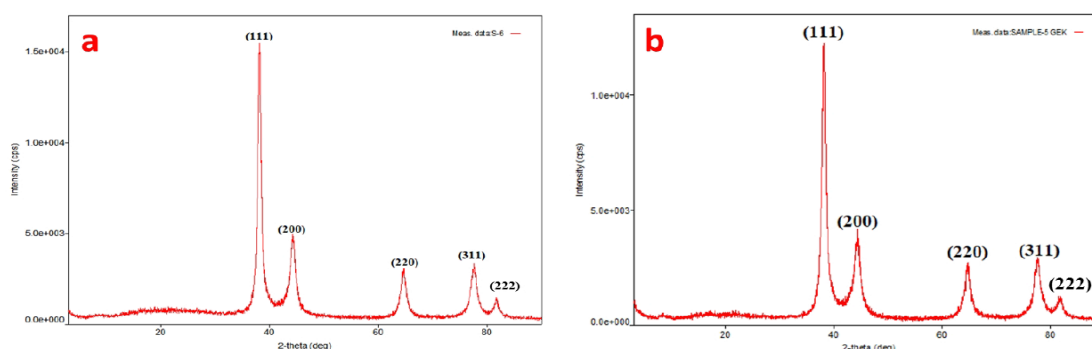


**Figure 4.** XRD pattern of biologically synthesized (a) AuNPs/GI and (b) AuNPs/GC.

Scherrer constant,  $\lambda$  is the X-ray radiation wavelength (1.54 Å),  $\beta$  is the full width at half maximum (FWHM) intensity of the diffraction peaks of (1 1 1) Bragg reflection, and  $\theta$  is the diffraction angle. From the calculations, the average particle sizes of synthesized AuNPs were found to be 11 nm and 8 nm for AuNPs/GI and AuNPs/GC respectively, which were found close to the average particle size ~10 nm measured using HR-TEM.

#### EDX analysis

The compositional analysis of AuNPs was studied using EDX analysis as shown in Figure 5(a) and 5(b). EDX spectrum illustrated the presence of the Au at 1.5 keV for AuNPs/GI and at 2.2 keV for AuNPs/GC. The elemental compositions of Au in AuNPs/GI and AuNPs/GC were found to be 53.49 % and 57.36 % respectively. Other weak/moderate signals, i.e. C, O, K, Ca, and Cl were also observed; this may arise from plant extract that bound to the surface of AuNPs or were present in the vicinity of the particles for the stabilization of the nanoparticles.<sup>78</sup>

#### HR-TEM analysis

HR-TEM analysis is one of the important techniques which gives information about the average particle size, and particle size distribution of synthesized NPs. The synthesized AuNPs are mostly spherical with

a triangular shape, the average sizes of the AuNPs were ranging from 2 – 10 nm and it was found to be in good agreement with the particle size of 8 – 11 nm determined using XRD analysis. The crystallinity of AuNPs evidenced by the XRD pattern was further confirmed by selected area electron diffraction (SAED) which accounted for bright circular rings that were indexed to the FCC structure of AuNPs [Figures 6(a-d) and 7(a-d)].

#### DPPH free radical scavenging activity

The human body during the respiration process produces harmful free radicals *viz.* reactive oxygen species (ROS), reactive nitrogen species (RNS), and reactive sulfur species (RSS).<sup>79</sup> Active phytoconstituents such as phenolics and flavonoids play an important role to neutralize these harmful free radicals in the human body. DPPH is a violet-colored, stable free radical which turns yellow when gets scavenged by a scavenger typically by an antioxidant compound. Radical scavenging assay by DPPH free radical was used to evaluate the antioxidant activity of synthesized AuNPs. The AuNPs showed 51.05 % (GI) and 44.05 % (GC) scavenging activity compared with standard ascorbic acid (94.11 %) at 100 µg/ml concentration. Aqueous extracts of GI and GC showed 45.90 % and 36.49 % inhibition respectively at 100 µg/ml, which is comparably lower than that of AuNPs (Figure 8). The

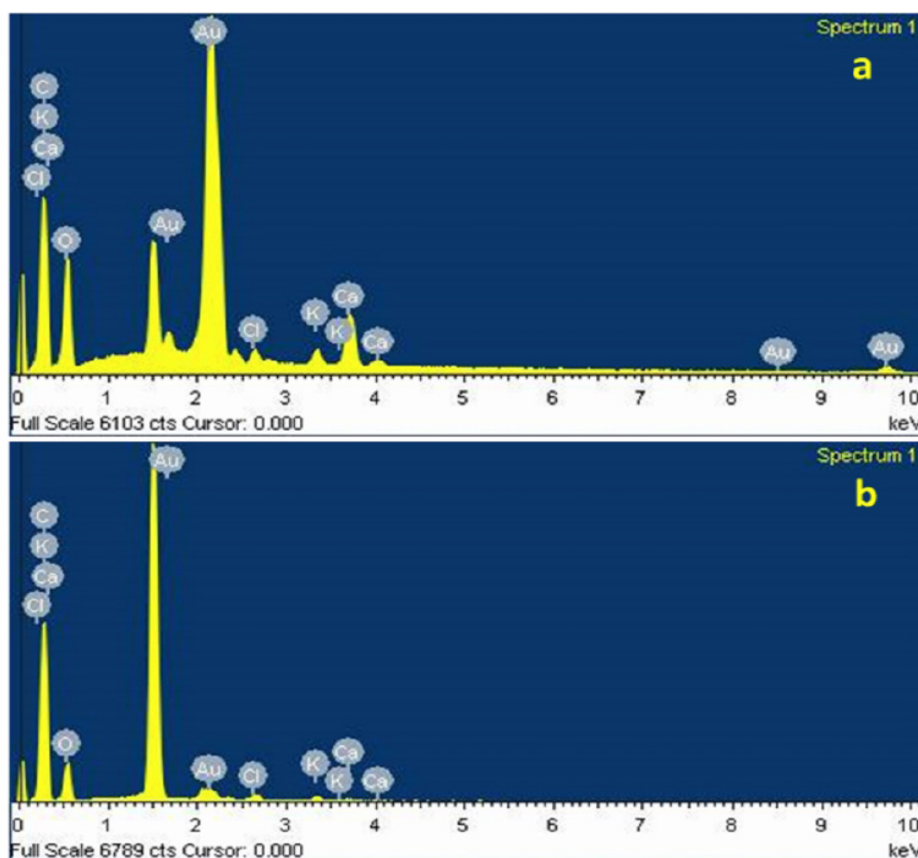
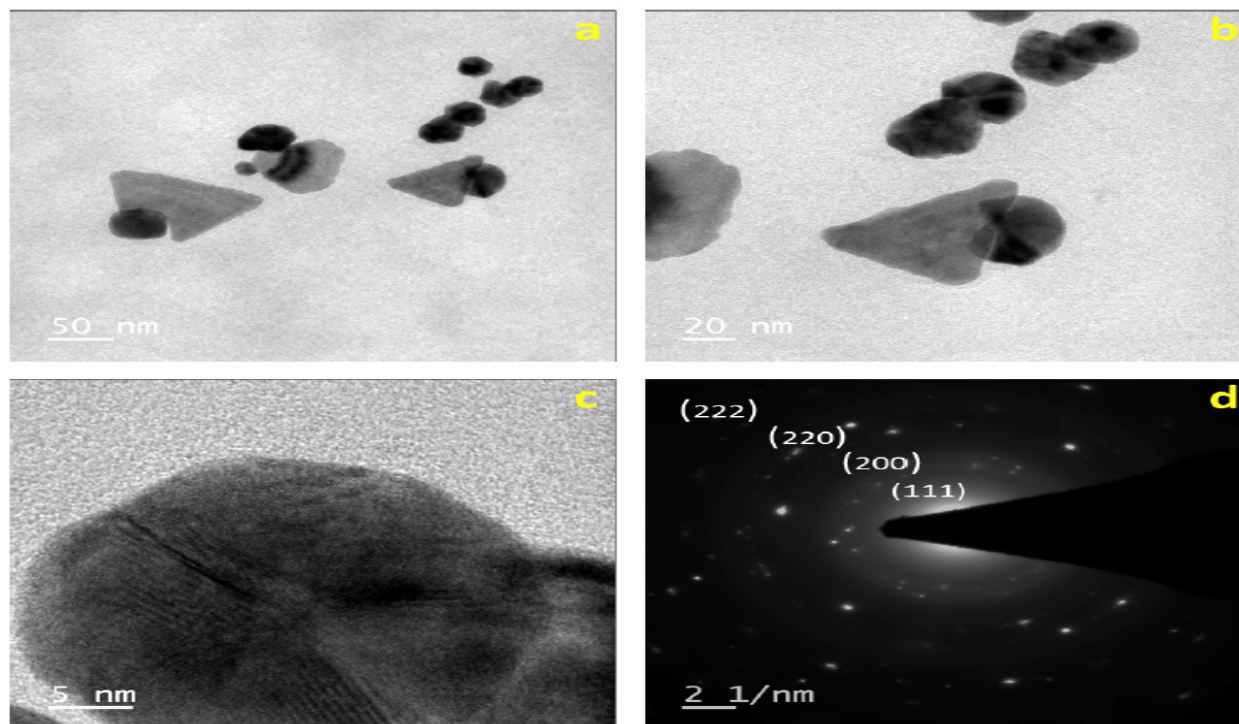
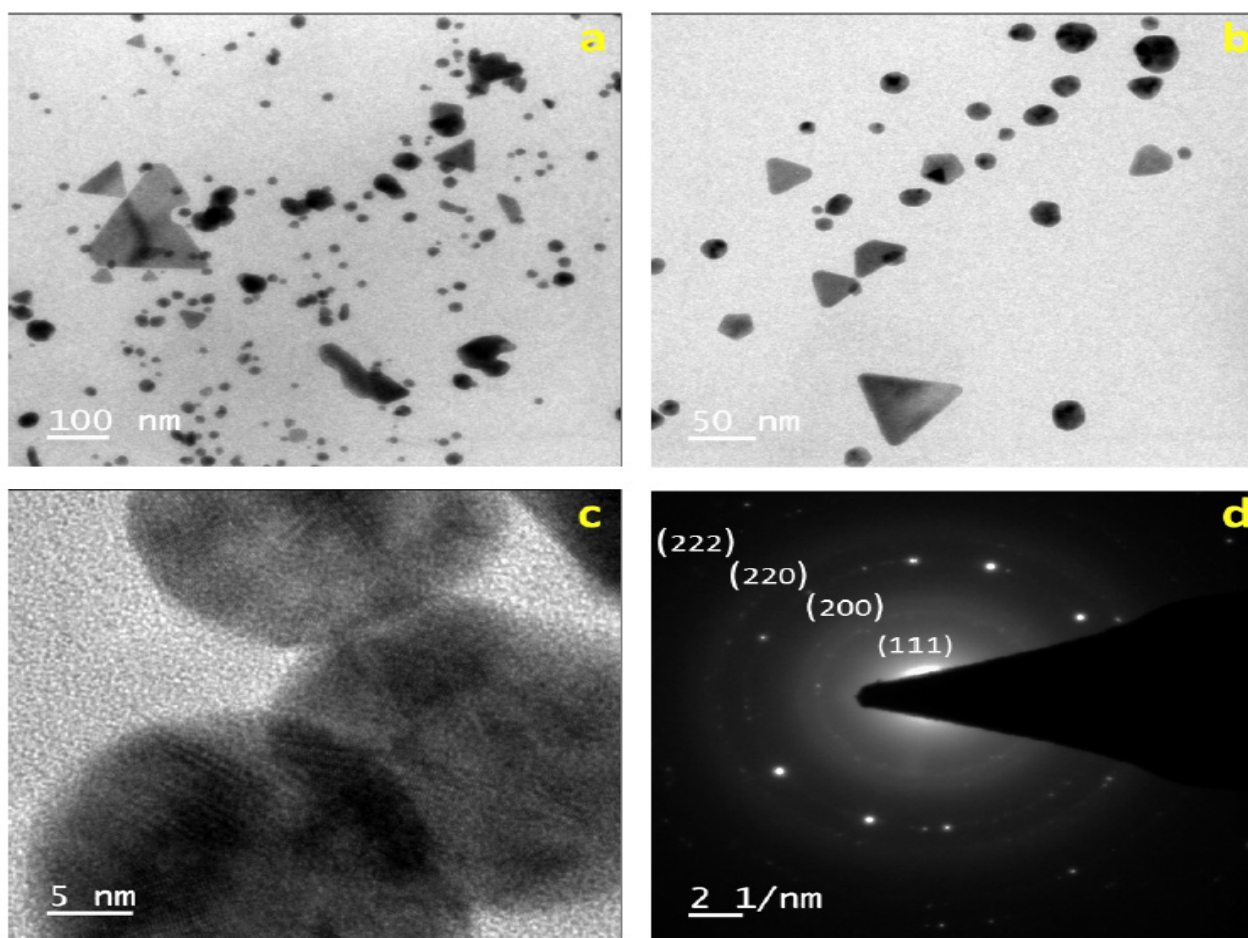


Figure 5. EDX spectrum of synthesized (a) AuNPs/GI and (b) AuNPs/GC.



**Figure 6.** (a), (b), (c) are HR-TEM and (d) SAED images of synthesized AuNPs/GI.



**Figure 7.** (a), (b), (c) are HR-TEM and (d) SAED images of synthesized AuNPs/GC.

DPPH free radical scavenging activity was found to be more in AuNPs/GI compared to AuNPs/GC. The free radical scavenging activities of the AuNPs can be attributed to the presence of functional groups of various secondary metabolites involved in the synthesis NPs.

**Cytotoxic activity**

An MTT was performed to investigate the cytotoxic activity of the synthesized AuNPs. As presented in Figure 9(a) and 9(b), biogenic AuNPs, the concentration required to cause 50 % cell death was more than standard drug doxorubicin ( $IC_{50} = 38.75 \mu\text{g/ml}$ ).  $IC_{50}$  values of AuNPs mediated through GI and GC were found to be  $34.55 \mu\text{g/ml}$  and  $35.69 \mu\text{g/ml}$  respectively for the MCF-7 cancer cell line. An

inverted microscope was used to study morphology at different time intervals (Figure 10).

**Antibacterial activity**

There are various perspectives on the antibacterial activity of AuNPs. The principle mechanism by which NPs exhibit antibacterial action may be through oxidative stress created by ROS. This factor can destroy proteins and DNA in bacteria. AuNPs have good chemical stability, increased surface area, and small size which boost faster association with microorganisms.<sup>80,81</sup>

In the present investigation, the average ZOI for AuNPs/GI and AuNPs/GC showed 9 mm and 13 mm for *B. subtilis* when compared to 10 mm and 12 mm for *E. coli*. The average ZOI values for GI extract were found to be 6 mm and 5 mm; for GC extract were 4 mm and 6 mm for *B. subtilis*

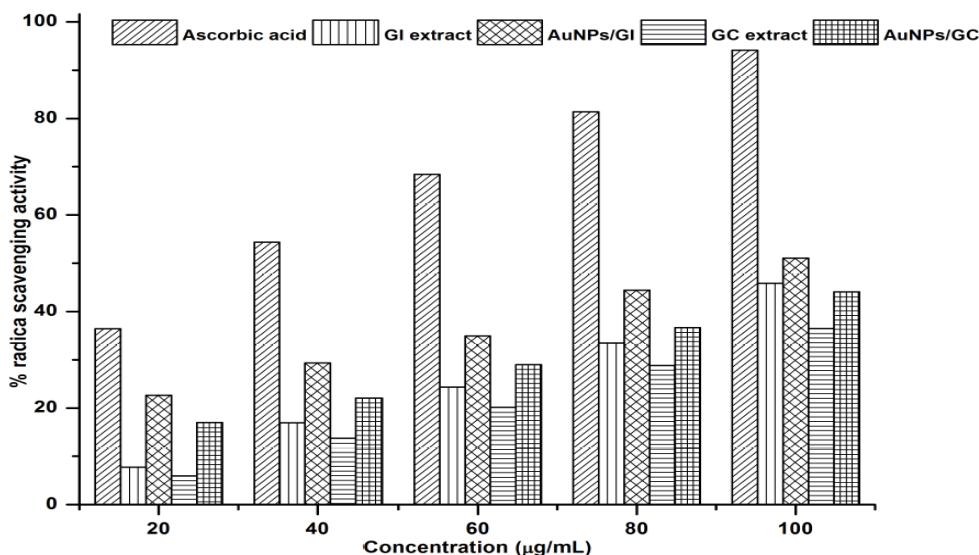


Figure 8. DPPH free radical scavenging activity.

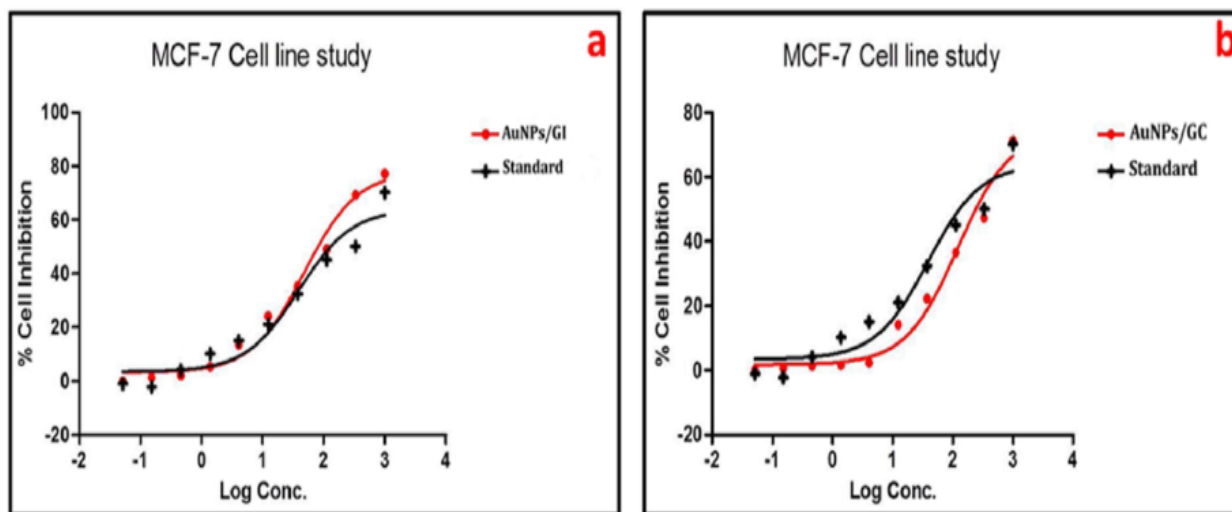
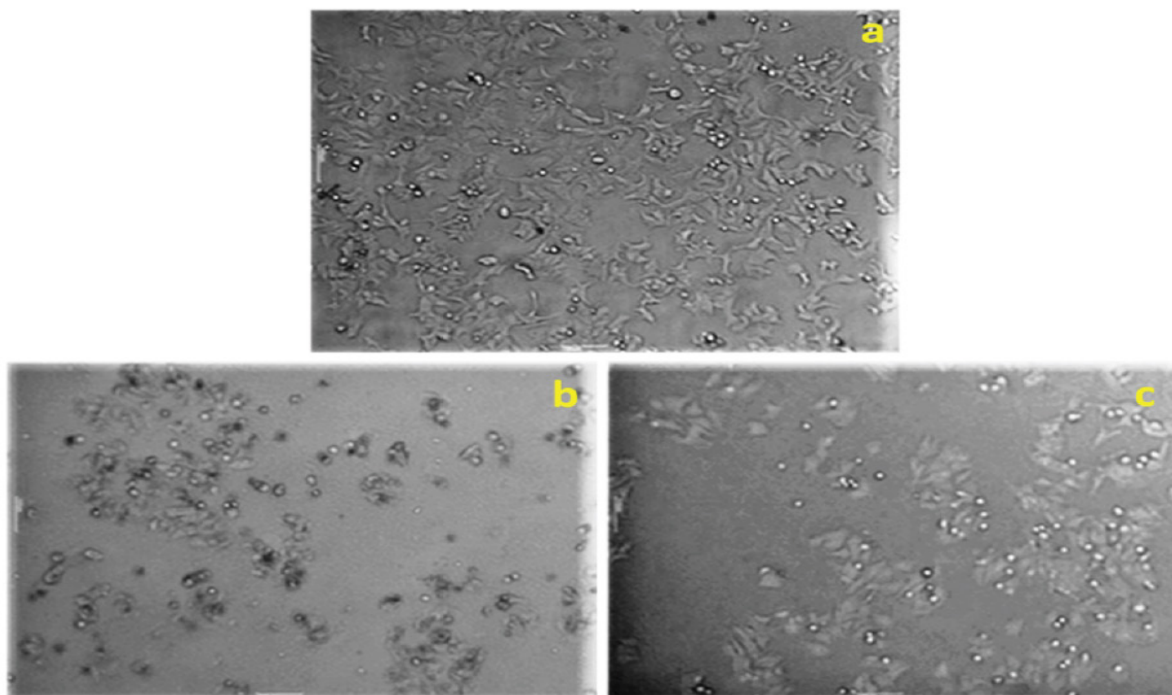


Figure 9. Cell viability (a) AuNPs/GI (b) AuNPs/GC of human breast cancer cell lines (MCF-7) after treatment with various concentrations (0.05-1000 µg/ml).





**Figure 10.** Microscopic images of (a) Control (b) MCF-7 cells after treatment with AuNPs/GI and (c) MCF-7 cells after treatment with AuNPs/GC.

and *E. coli* respectively (Table 2). Figure 11 shows ZOI on bacteria due to the effect of synthesized AuNPs. Contrary to anticancer activity, the antibacterial property also did not show any linear relationship between antioxidant

activity and total phenolics of AuNPs mediated through aqueous extracts of GI and GC in respect of percentage free radical scavenging capacity and ZOI. The zone of inhibition of AuNPs is far better than aqueous extracts.

**Table 2.** Antibacterial activity of *Garcinia*-mediated AuNPs against two pathogenic bacteria (zone of inhibition in mm).

| Bacterial strains  | Average ZOI (mm) |          |            |          | Control |
|--------------------|------------------|----------|------------|----------|---------|
|                    | GI extract       | AuNPs/GI | GC extract | AuNPs/GC |         |
| <i>B. subtilis</i> | 6                | 9        | 4          | 13       | 14      |
| <i>E. coli</i>     | 5                | 10       | 6          | 12       | 16      |

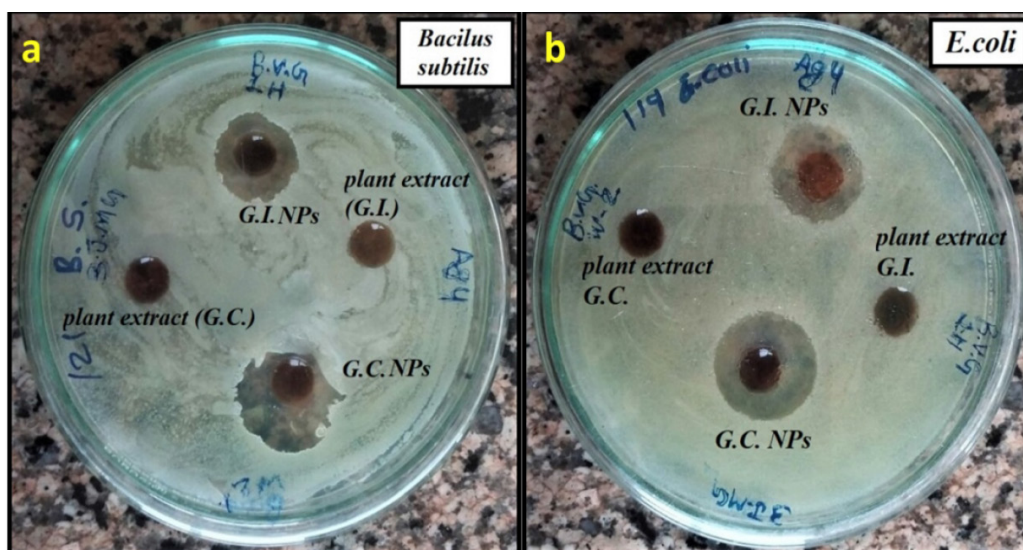


**Figure 11.** Culture plate showing antibacterial activity AuNPs against (a) *B. subtilis* (b) *E. coli*.

## Conclusion

We have reported the one-pot green synthesis of AuNPs using aqueous extract of pericarp powder of two commercial and therapeutically important *Garcinia* species. The availed method for the synthesis of AuNPs is simple, eco-friendly, and cost-effective. FT-IR spectroscopy recommended the involvement of mainly phenolic compounds in the synthesis. The synthesized AuNPs were spherical and triangular and the average sizes of AuNPs were found to be 2–10 nm by HR-TEM, which is in good agreement with the particle size of 8–11 confirmed by XRD analysis. The cytotoxicity and antibacterial properties showed a positive linear relationship between antioxidant activity and total phenolics of AuNPs indicating the crucial role of the antioxidants/phenolics of the GI/GC extracts on anticancer and antibacterial activity. AuNPs showed promising cytotoxicity against MCF-7 cancer cell lines with  $IC_{50}$  values 34.55  $\mu\text{g/ml}$  and 35.69  $\mu\text{g/ml}$  for AuNPs/GI and AuNPs/GC, respectively which is better than that of standard drug doxorubicin. Dissimilarity in biological property of AuNPs mediated through aqueous fruits pericarp extracts of GI and GC recommending the effect of phytoconstituents on the functionality/ physico-chemical properties of AuNPs. It is needed to explore the exact mechanism of synthesis of AuNPs and also to perceive the precise role of phytochemicals involved in the reduction and stabilization of AuNPs. Furthermore, it is superficially promising; the large-scale production of AuNPs expending plant extracts has not been achieved so far. The biocompatibility of the synthesized AuNPs has to be well documented regularly for a better understanding of their fortune in the human body.

## Acknowledgments

One of the authors Azazahamad A. Kureshi (Senior Research Fellow, UGC-MANF) gratefully acknowledges the University Grants Commission (UGC) and Ministry of Minority Affairs, New Delhi, Govt. of India for providing financial assistance (Award No:2015-16/MANF-2015-17-GUJ-49309). Authors (SK and RS) acknowledge ICAR, New Delhi for funding a research project "Network Project on High Value Compounds/Phytochemicals".

## Author Contributions

AAK: Performed characterization and biological assays part, HMV: Synthesis of AuNPs, SK: Drafting of the work and critically reviewed the manuscript, RS: Analyzed the data, PL: Conceptualized the work and also written the manuscript. All authors have read and agreed to the published version of the manuscript.

## Conflict of Interests

The authors declare that there are no conflicts of interest.

## References

1. Narayanan KB, Sakthivel N. Phytosynthesis of gold

nanoparticles using leaf extract of *Coleus amboinicus* Lour. Mater Charact. 2010;61(11):1232-8. doi:10.1016/j.matchar.2010.08.003

2. Aswathy Aromal S, Philip D. Facile one-pot synthesis of gold nanoparticles using tannic acid and its application in catalysis. Phys. E Low-Dimensional Syst. Nanostructures. 2012;44(7-8):1692-6. doi:10.1016/j.physe.2012.04.022
3. Shashanka R, Karaoglanli AC, Ceylan Y, Uzun O, Rajendrachari S. A fast and robust approach for the green synthesis of spherical magnetite ( $\text{Fe}_3\text{O}_4$ ) Nanoparticles by *Tilia tomentosa* (Ihlamur) leaves and its antibacterial studies. Pharm Sci. 2020;26(2):175-83. doi:10.34172/PS.2020.5
4. Mishra A, Kumari M, Pandey S, Chaudhry V, Gupta KC, Nautiyal CS. Biocatalytic and antimicrobial activities of gold nanoparticles synthesized by *Trichoderma* sp. Bioresour Technol. 2014;166:235-42. doi:10.1016/j.biortech.2014.04.085
5. Shashanka R, Swamy BK, Reddy S, Chaira D. Synthesis of silver nanoparticles and their applications. Anal Bioanal Electrochem. 2013;1:455-66.
6. Reddy S, Kumara Swamy BE, Aruna S, Kumar M, Shashanka R, Jayadevappa H. Preparation of NiO/ZnO hybrid nanoparticles for electrochemical sensing of dopamine and uric acid. Chem Sensors. 2012;2:7.
7. Shashanka R. Effect of sintering temperature on the pitting corrosion of ball milled duplex stainless steel by using linear sweep voltammetry. Anal Bioanal Electrochem. 2018;10:349-361.
8. Shashanka R, Chaira D, Kumara Swamy BE. Electrochemical investigation of duplex stainless steel at carbon paste electrode and its application to the detection of dopamine, ascorbic, and uric acid. Int J Sci Eng Res. 2015;6(9):1863-71.
9. Shashanka R, Kumara Swamy BE. Simultaneous electro-generation and electro-deposition of copper oxide nanoparticles on glassy carbon electrode and its sensor application. SN Appl Sci. 2020;2(5):1-10. doi:10.1007/s42452-020-2785-1
10. Shashanka R, Esgin H, Yilmaz VM, Caglar Y. Fabrication and characterization of green synthesized ZnO nanoparticle based dye-sensitized solar cell. J Sci Adv Mater Devices. 2020;5:185-91. doi:10.1016/j.jsamd.2020.04.005
11. Shashanka R, Yilmaz VM, Karaoglanli AC, Uzun O. Investigation of activation energy and antibacterial activity of CuO nano-rods prepared by *Tilia tomentosa* (Ihlamur) leaves. Mor J Chem. 2020;8(2):497-509. doi:10.48317/IMIST.PRSM/morjchem-v8i2.17765
12. Shashanka R, Chaira D, Kumara Swamy B. Fabrication of yttria dispersed duplex stainless steel electrode to determine dopamine, ascorbic and uric acid electrochemically by using cyclic voltammetry. Int J Sci Eng Res. 2016;7(3):1275-85.
13. Shashanka R. Non-lubricated dry sliding wear behavior of spark plasma sintered nano-structured stainless

- steel. *J Mater Environ Sci*. 2019;10(8):767-77.
14. Shashanka R, Ceylan KB. The activation energy and antibacterial investigation of spherical Fe<sub>3</sub>O<sub>4</sub> nanoparticles prepared by *Crocus sativus* (Saffron) flowers. *Biointerface Res App Chem*. 2020;10:5951-9. doi:10.33263/BRIAC104.951959
  15. Shashanka R, Kumara Swamy BE. Biosynthesis of silver nanoparticles using leaves of *Acacia melanoxylon* and their application as dopamine and hydrogen peroxide sensors. *Phy Chem Res*. 2020;8(1):1-18. doi:10.22036/pcr.2019.205211.1688
  16. Shashanka R, Kumara Swamy BE. Simultaneous electro-generation and electro- Pan Y, Neuss S, Leifert A, Fischler M, Wen F, Simon U, et al. Size-dependent cytotoxicity of gold nanoparticles. *Small*. 2007;3(11):1941-9. doi:10.1002/smll.200700378
  17. Shankar SS, Rai A, Ankamwar B, Singh A, Ahmad A, Sastry M. Biological synthesis of triangular gold nanoprisms. *Nature Mater*. 2004;3(7):482-8. doi:10.1038/nmat1152
  18. Bhattacharya R, Mukherjee P. Biological properties of “naked” metal nanoparticles. *Adv Drug Del Rev*. 2008;60(11):1289-306. doi:10.1016/j.addr.2008.03.013
  19. Khan A, Rashid A, Younas R, Chong R. A chemical reduction approach to the synthesis of copper nanoparticles. *Int Nano Lett*. 2016;6(1):21-6. doi:10.1007/s40089-015-0163-6
  20. Jun G, Liping J, Junjie Z. Crystal formation and growth mechanism of inorganic nanomaterials in sonochemical syntheses. *Sci China Chem*. 2012;55(11):2292-310. doi:10.1007/s11426-012-4732-5
  21. Jadhav S, Gaikwad S, Nimse M, Rajbhoj A. Copper oxide nanoparticles: synthesis, characterization and their antibacterial activity. *J Cluster Sci*. 2011;22(2):121-9. doi:10.1007/s10876-011-0349-7
  22. Shah M, Fawcett D, Sharma S, Tripathy SK, Poinern GEJ. Green synthesis of metallic nanoparticles via biological entities. *Materials*. 2015;8(11):7278-308. doi:10.3390/ma8115377
  23. Irvani S, Korbekandi H, Zolfaghari B. Synthesis of silver nanoparticles : chemical, physical and biological methods synthesis of silver NPs. *Res Pharma Sci*. 2013;9(6):385-406.
  24. Li X, Xu H, Chen Z-S, Chen G. Biosynthesis of nanoparticles by microorganisms and their applications. *J Nanomat*. 2011;2011:270974. doi:10.1155/2011/270974
  25. U Picoli S, Durán M, F Andrade P, Duran N. Silver nanoparticles/silver chloride (Ag/AgCl) synthesized from *Fusarium oxysporum* acting against *Klebsiella pneumoniae* carbapenemase (KPC) and extended spectrum beta-lactamase (ESBL). *Frontiers Nanosci Nanotechnol*. 2016;2(2):107-10. doi:10.15761/fnn.1001117
  26. Irvani S. Green synthesis of metal nanoparticles using plants. *Green Chem*. 2011;13(10):2638-50. doi:10.1039/c1gc15386b
  27. Patil MP, Palma J, Simeon NC, Jin X, Liu X, Ngabire D, et al. *Sasa borealis* leaf extract-mediated green synthesis of silver-silver chloride nanoparticles and their antibacterial and anticancer activities. *New J Chem*. 2017;41(3):1363-71. doi:10.1039/c6nj03454c
  28. Stalin Dhas T, Ganesh Kumar V, Karthick V, Jini Angel K, Govindaraju K. Facile synthesis of silver chloride nanoparticles using marine alga and its antibacterial efficacy. *Spectrochim Acta A*. 2014;120:416-20. doi:10.1016/j.saa.2013.10.044
  29. Kuppusamy P, Yusoff MM, Maniam GP, Govindan N. Biosynthesis of metallic nanoparticles using plant derivatives and their new avenues in pharmacological applications – An updated report. *Saudi Pharm J*. 2016;24(4):473-84. doi:10.1016/j.jsps.2014.11.013
  30. Suman TY, Radhika Rajasree SR, Ramkumar R, Rajthilak C, Perumal P. The Green synthesis of gold nanoparticles using an aqueous root extract of *Morinda citrifolia* L. *Spectrochim Acta A*. 2014;118:11-6. doi:10.1016/j.saa.2013.08.066
  31. Krishnaraj C, Muthukumar P, Ramachandran R, Balakumaran MD, Kalaichelvan PT. *Acalypha indica* Linn: Biogenic synthesis of silver and gold nanoparticles and their cytotoxic effects against MDA-MB-231, human breast cancer cells. *Biotechnol Rep*. 2014;4(1):42-9. doi:10.1016/j.btre.2014.08.002
  32. Noruzi M. Biosynthesis of gold nanoparticles using plant extracts. *Bioproc Biosyst Eng*. 2015;38(1):1-14. doi:10.1007/s00449-014-1251-0
  33. Rathore M, Mohanty IR, Maheswari U, Dayal N, Suman R, Joshi DS. Comparative *in vivo* assessment of the subacute toxicity of gold and silver nanoparticles. *J Nanopart Res*. 2014;16(4):1-12. doi:10.1007/s11051-014-2338-x
  34. Allafchian AR, Mirahmadi-Zare SZ, Jalali SAH, Hashemi SS, Vahabi MR. Green synthesis of silver nanoparticles using phlomis leaf extract and investigation of their antibacterial activity. *J Nanostructure Chem*. 2016;6(2):129-35. doi:10.1007/s40097-016-0187-0
  35. Manjari G, Saran S, Arun T, Devipriya SP, Vijaya Bhaskara Rao A. Facile *Aglaia elaeagnoides* mediated synthesis of silver and gold nanoparticles: antioxidant and catalysis properties. *J Cluster Sci*. 2017;28(4):2041-56. doi:10.1007/s10876-017-1199-8
  36. Abdullah NISB, Ahmad MB, Shameli K. Biosynthesis of silver nanoparticles using *Artocarpus elasticus* stem bark extract. *Chem Central J*. 2015;9(1):1-7. doi:10.1186/s13065-015-0133-0
  37. Kumar A, Das N, Satija NK, Mandrah K, Roy SK, Rayavarapu RG. A novel approach towards synthesis and characterization of non-cytotoxic gold nanoparticles using taurine as capping agent. *Nanomaterials*. 2020;10(1):45. doi:10.3390/nano10010045
  38. Abraham Z, Malik SK, Rao GE, Narayanan SL, Biju S. Collection and characterisation of Malabar tamarind [*Garcinia cambogia* (Gaertn.) Desr.]. *Genet Resour*

- Crop Evol. 2006;53(2):401-6. doi:10.1007/s10722-004-0584-y
39. Gustafson KR, Blunt JW, Munro MH, Fuller RW, McKee TC, et al. The guttiferones, HIV-inhibitory benzophenones from *Symphonia globulifera*, *Garcinia livingstonei*, *Garcinia ovalifolia* and *Clusia rosea*. Tetrahedron, 1992;48:10093-102. doi:10.1016/S0040-4020(01)89039-6
  40. Shara M, Ohia SE, Schmidt RE, Yasmin T, Zardetto-Smith A, Kincaid A, et al. Physico-chemical properties of a novel (-)-hydroxy- citric acid extract and its effect on body weight, selected organ weights, hepatic lipid peroxidation and DNA fragmentation, hematology and clinical chemistry, and histopathological changes over a period of 90 days. 2004;260:171-86. doi:10.1023/B:MCBI.0000026069.53960.75
  41. Deepak V. Nature watch. Resonance. 2015;20(1):47-54. doi:10.1007/s12045-015-0152-0
  42. Deodhar S, Pawar K, Singh N, Thengane RJ, Thengane SR. Clonal propagation of female plants of *Garcinia indica* Choiss: a tree species of high medicinal value. J Appl Biol Biotechnol. 2015;2(6):18-25. doi:10.7324/jabb.2014.2605
  43. Jayaprakasha GK, Sakariah KK. Determination of organic acids in leaves and rinds of *Garcinia indica* (Desr.) by LC. J Pharm Biomed Anal. 2002;28(2):379-84. doi:10.1016/s0731-7085(01)00623-9
  44. Nayak CA, Srinivas P, Rastogi NK. Characterisation of anthocyanins from *Garcinia indica* Choisy. Food Chem. 2010;118(3):719-24. doi:10.1016/j.foodchem.2009.05.052
  45. Kureshi AA, Dholakiya C, Hussain T, Mirgal A, Salvi SP, Barua PC, et al. Simultaneous identification and quantification of three xanthenes and two polyisoprenylated benzophenones in eight Indian *Garcinia* species using a validated UHPLC-PDA Method. J AOAC Int. 2019;102(5):1423-34. doi:10.5740/jaoacint.18-0335
  46. Kureshi AA, Hussain T, Mirgal A, Salvi SP, Barua PC, Talukdar M, et al. Comparative evaluation of antioxidant properties of extracts of fruit rinds of *Garcinia* species by in vitro assays. Indian J Hort. 2019;76(2):338-43. doi:10.5958/0974-0112.2019.00053.7
  47. Jagtap P, Road KBH, Campus A. Phytochemical characterization and cytotoxic evaluation of methanolic extract of *Garcinia indica* fruit rind. Int J Pharmacogn. 2017;4(11):372-7. doi:10.13040/IJPSR.0975-8232.IJP.4(11).372-77
  48. Ajay S, Rajesh S, Pandey V, Golhani D, Jain C. P. In-Vitro Antioxidant activity of *Garcinia cambogia* fruits. J Med Pharm Allied Sci. 2014;03:67-73.
  49. Roy S, Rink C, Khanna S, Phillips C, Bagchi D, Bagchi M, et al. Body weight and abdominal fat gene expression profile in response to a novel hydroxycitric acid-based dietary supplement. Gene Expr. 2003;11(5-6):251-62. doi:10.3727/000000003783992289
  50. Tharachand, Selvaraj I, Avadhani M. Medicinal properties of Malabar tamarind [*Garcinia cambogia* (Gaertn.) DESR.]. Int J Pharm Sci Rev Res. 2013;19(2):101-7.
  51. Park JS, Ahn EY, Park Y. Asymmetric dumbbell-shaped silver nanoparticles and spherical gold nanoparticles green-synthesized by mangosteen (*Garcinia mangostana*) pericarp waste extracts. Int J Nanomed. 2017;12:6895-908. doi:10.2147/IJN.S140190
  52. Rajakannu S, Shankar S, Perumal S, Subramanian S, Dhakshinamoorthy GP. Biosynthesis of silver nanoparticles using *Garcinia mangostana* fruit extract and their antibacterial, antioxidant activity. Int J Curr Microbiol Appl Sci. 2015;4(1):944-52.
  53. Lee KX, Shameli K, Miyake M, Khairudin NB, Mohamad SE, Hara H, et al. Gold Nanoparticles Biosynthesis: A simple route for control size using waste peel extract. IEEE Trans Nanotechnol. 2017;16(6):954-7. doi:10.1109/TNANO.2017.2728600
  54. Nishanthi R, Malathi S, Palani P. Green synthesis and characterization of bioinspired silver, gold and platinum nanoparticles and evaluation of their synergistic antibacterial activity after combining with different classes of antibiotics. Mater Sci Eng C. 2019;96:693-707. doi:10.1016/j.msec.2018.11.050
  55. Xin Lee K, Shameli K, Miyake M, Kuwano N, Bt Ahmad Khairudin NB, et al. Green synthesis of gold nanoparticles using aqueous extract of *Garcinia mangostana* fruit peels. J Nanomat. 2016;2016: 8489094. doi:10.1155/2016/8489094
  56. Hazarika M, Borah D, Bora P, Silva AR, Das P. Biogenic synthesis of palladium nanoparticles and their applications as catalyst and antimicrobial agent. PLoS ONE. 2017;12(9):1-19. doi:10.1371/journal.pone.0184936
  57. Sangaonkar GM, Pawar KD. *Garcinia indica* mediated biogenic synthesis of silver nanoparticles with antibacterial and antioxidant activities. Colloids Surf B. 2018;164:210-7. doi:10.1016/j.colsurfb.2018.01.044
  58. Aminuzzaman M, Ying LP, Goh W-S, Watanabe A. Green synthesis of zinc oxide nanoparticles using aqueous extract of *Garcinia mangostana* fruit pericarp and their photocatalytic activity. Bull Mater Sci. 2018;41(2):50. doi:10.1007/s12034-018-1568-4
  59. Ramkumar SS, Sivakumar N, Selvakumar G, Selvakumar T, Sudhakar C, Ashokkumar B, et al. Green synthesized silver nanoparticles from: *Garcinia imberti* bourd and their impact on root canal pathogens and HepG2 cell lines. RSC Adv. 2017;7(55):34548-55. doi:10.1039/c6ra28328d
  60. Desai MP, Sangaokar GM, Pawar KD. Kokum fruit mediated biogenic gold nanoparticles with photoluminescent, photocatalytic and antioxidant activities. Process Biochem. 2018;70:188-97. doi:10.1016/j.procbio.2018.03.027
  61. Syed B, Bisht N, Bhat PS, Nikhil KR, Prasad A, Dhananjaya BL, et al. Phytogenic synthesis of

- nanoparticles from *Rhizophora mangle* and their bactericidal potential with DNA damage activity. *Nano-Structures Nano-Obj.* 2017;10:112-5. doi:10.1016/j.nanoso.2017.03.011
62. Raghavendra M, Yatish KV, Lalithamba HS. Plant-mediated green synthesis of ZnO nanoparticles using *Garcinia gummi-gutta* seed extract: Photoluminescence, screening of their catalytic activity in antioxidant, formylation and biodiesel production. *Eur Phys J Plus.* 2017;132(8):358. doi:10.1140/epjp/i2017-11627-1
  63. Rajan A, Meenakumari M, Philip D. Shape tailored green synthesis and catalytic properties of gold nanocrystals. *Spectrochim Acta A.* 2014;118:793-9. doi:10.1016/j.saa.2013.09.086
  64. Krishnaprabha M, Pattabi M. Synthesis of gold nanoparticles using *Garcinia indica* fruit rind extract. *Int J Nanosci.* 2016;15(05n06):1660015. doi:10.1142/s0219581x16600152
  65. Moshalagae Motlatle A, Kesavan Pillai S, Rudolf Scriba M, Sinha Ray S. Chemical synthesis, characterization and evaluation of antimicrobial properties of Cu and its oxide nanoparticles. *J Nanopart Res.* 2016;18(10):312. doi:10.1007/s11051-016-3614-8
  66. Das D, Nath BC, Phukon P, Dolui SK. Synthesis and evaluation of antioxidant and antibacterial behavior of CuO nanoparticles. *Colloids Surf B.* 2013;101:430-3. doi:10.1016/j.colsurfb.2012.07.002
  67. Yallappa S, Manjanna J, Sindhe MA, Satyanarayan ND, Pramod SN, Nagaraja K. Microwave assisted rapid synthesis and biological evaluation of stable copper nanoparticles using *T. arjuna* bark extract. *Spectrochim Acta A.* 2013;110:108-15. doi:10.1016/j.saa.2013.03.005
  68. Wang W, Tang Q, Yu T, Li X, Gao Y, Li J, et al. Surfactant-free preparation of Au@Resveratrol hollow nanoparticles with photothermal performance and antioxidant activity. *ACS Appl Mater Interfaces.* 2017;9(4):3376-87. doi:10.1021/acscami.6b13911
  69. Černík M, Thekkae Padil VV. Green synthesis of copper oxide nanoparticles using gum karaya as a biotemplate and their antibacterial application. *Int J Nanomed.* 2013;8(1):889-98. doi:10.2147/ijn.s40599
  70. Naika HR, Lingaraju K, Manjunath K, Kumar D, Nagaraju G, Suresh D, et al. Green synthesis of CuO nanoparticles using *Gloriosa superba* L. extract and their antibacterial activity. *J Taibah Univ Sci.* 2015;9(1):7-12. doi:10.1016/j.jtusci.2014.04.006
  71. Vilas V, Philip D, Mathew J. Biosynthesis of Au and Au/Ag alloy nanoparticles using *Coleus aromaticus* essential oil and evaluation of their catalytic, antibacterial and antiradical activities. *J Mol Liq.* 2016;221:179-89. doi:10.1016/j.molliq.2016.05.066
  72. Abdelhamid AA, Al-Ghobashy MA, Fawzy M, Mohamed MB, Abdel-Mottaleb MMSA. Phytosynthesis of Au, Ag, and Au-Ag bimetallic nanoparticles using aqueous extract of sago pondweed (*Potamogeton pectinatus* L.). *ACS Sustain Chem Eng.* 2013;1(12):1520-9. doi:10.1021/sc4000972
  73. Mulvaney P. Surface plasmon spectroscopy of nanosized metal particles. *Langmuir.* 2002;12(3):788-800. doi:10.1021/la9502711
  74. Nur H, Md. Nasir S. Gold nanoparticles embedded on the surface of polyvinyl alcohol layer. *Mal J Fund Appl Sci.* 2008;4(1):245-52. doi:10.11113/mjfas.v4n1.33
  75. Geetha MS, Nagabhushana H, Shivananjaiah HN. Green mediated synthesis and characterization of ZnO nanoparticles using *Euphorbia jatropa* latex as reducing agent. *J Sci Adv Mater Dev.* 2016;1(3):301-10. doi:10.1016/j.jsamd.2016.06.015
  76. Kalyan Kamal SS, Vimala J, Sahoo PK, Ghosal P, Ram S, Durai L. A green chemical approach for synthesis of shape anisotropic gold nanoparticles. *Int Nano Lett.* 2014;4:109. doi:10.1007/s40089-014-0109-4
  77. Balavigneswaran CK, Sujin Jeba Kumar T, Moses Packiaraj R, Prakash S. Rapid detection of Cr(VI) by AgNPs probe produced by *Anacardium occidentale* fresh leaf extracts. *Appl Nanosci.* 2014;4(3):367-78. doi:10.1007/s13204-013-0203-3
  78. Lee SY, Krishnamurthy S, Cho CW, Yun YS. Biosynthesis of gold nanoparticles using *Ocimum sanctum* extracts by solvents with different polarity. *ACS Sustain Chem Engg.* 2016;4(5):2651-9. doi:10.1021/acssuschemeng.6b00161
  79. Rajan A, Vilas V, Philip D. Studies on catalytic, antioxidant, antibacterial and anticancer activities of biogenic gold nanoparticles. *J Mol Liq.* 2015;212:331-9. doi:10.1016/j.molliq.2015.09.013
  80. Sreekanth TVM, Nagajyothi PC, Supraja N, Prasad TNVKV. Evaluation of the antimicrobial activity and cytotoxicity of phytogenic gold nanoparticles. *Appl Nanosci.* 2015;5(5):595-602. doi:10.1007/s13204-014-0354-x
  81. Nirmala Grace A, Pandian K. Antibacterial efficacy of aminoglycosidic antibiotics protected gold nanoparticles-A brief study. *Colloid Surface A.* 2007;297(1-3):63-70. doi:10.1016/j.colsurfa.2006.10.024